CrossMark

Characterization of coal using electron spin resonance: implications for the formation of inertinite macerals in the Witbank Coalfield, South Africa

Ofentse M. Moroeng[1,2] · Jonathan M. Keartland[3] · R. James Roberts[2] ·
Nicola J. Wagner[1]

Abstract Coal contains a significant concentration of free radicals as a result of the coalification process. One of the experimental methods sensitive to the presence of radicals is electron spin resonance (ESR), and differences in ESR spectra for different macerals may provide insight into coal-forming processes. In this study, ESR data along with the H/C atomic ratio (to infer the aromatic fraction) are used to characterize coal samples with the aim of assessing a fire-origin for dominant inertinite macerals. A medium rank C bituminous Witbank No. 4 Seam Upper coal (the parent) was density-fractionated to create vitrinite-rich and inertinite-rich samples. The parent sample consists of 42 vol% vitrinite and 49 vol% inertinite. The density-fractionated samples comprise of 81 vol% total vitrinite (dominated by collotelinite and collodetrinite), and 63 vol% total inertinite (dominated by fusinite, semifusinite, and inertodetrinite). The H/C ratio is 0.74 for the inertinite-rich sample, and 0.85 for the vitrinite-rich counterpart, suggesting the former sample is more aromatic. The ESR spectra obtained for the three samples were found to fit best using a Lorentzian distribution. The fit is noticeably better for the aromatic inertinite-rich sample, for which the spectrum is symmetric. This is attributed to pronounced electron mobility and exchange interactions. The higher radical content of the inertinite-rich and parent samples is attributed to the presence of specific inertinite macerals, namely: fusinite, semifusinite, and inertodetrinite. And, owing to the greater radical content of the inertinite-rich sample, the dominant inertinite macerals are interpreted to have formed through charring of plant matter.

Keywords Main Karoo Basin · Radical contents · Origin pathways · Charring · Fusinite · Semifusinite

1 Introduction

South African coals of the Main Karoo Basin, much like other Gondwana Permian coals, have high inertinite contents, comprised of a significant amount semifusinite and inertodetrinite (Falcon 1986a; Hagelskamp and Snyman

✉ Ofentse M. Moroeng
  marvinm@uj.ac.za

1 Department of Geology, University of Johannesburg,
   P.O. Box 524, Auckland Park 2006, South Africa

2 Department of Geology, University of Pretoria, Mineral
   Sciences Building, Pretoria 0002, South Africa

3 School of Physics and Materials Physics Institute, University
   of the Witwatersrand, Johannesburg 2050, South Africa

1988; Snyman 1989; Taylor et al. 1998; Glasspool 2003a, b; Van Niekerk et al. 2008, and references therein; Hower et al. 2012; O'Keefe et al. 2013). Inertinite has been shown to have higher carbon and lower hydrogen contents, as well as higher aromaticity than other maceral groups at the bituminous coal rank (Dyrkacz et al. 1984; Falcon 1986b; White et al. 1989; Maroto-Valer et al. 1994, 1998a; Davidson 2004; Van Niekerk et al. 2008; Van Niekerk and Mathews 2010; Moroeng et al. 2017). As a result, free radicals formed during coalification are better preserved (Retcofsky et al. 1968; Levine et al. 1982). Radical properties have been used to understand the origin and chemistry of organic matter globally, including coal and its constituent macerals (Austen et al. 1966; Retcofsky et al. 1968, 1981; Grandy and Petrakis 1979; Petrakis and Grandy 1981; Silbernagel et al. 1984a, b, 1986; Kwan and

Yen 1979; Fowler et al. 1987; Krevelen 1993, and references therein; Więckowski et al. 2000; Binet et al. 2002; Ikoma et al. 2002; Davidson 2004; Liu et al. 2014; Zhou et al. 2017). For South African coals, there appears to be no information available in the published literature regarding the use of electron spin resonance (ESR) to determine the properties of the coals.

According to Krevelen (1993), free radicals (i.e. unpaired electrons) in coal were discovered in 1954 by two research teams working independently. Following the discovery, there was an initial concerted focus on the origin and influence of the radicals on the chemical behaviour of coal in various technological applications (Austen et al. 1958, 1966; Retcofsky et al. 1968, 1981; Grandy and Petrakis 1979; Petrakis and Grandy 1981; Krevelen 1993, and references therein). An immediate observation made was that the radicals were primarily associated with the organic fraction of coal, rather than the mineral matter (Retcosfky et al. 1981).

In terms of elemental composition, coal is particularly distinctive from other fossil fuels: it has a significantly lower hydrogen and higher oxygen content in comparison to both petroleum and oil shale (Levine et al. 1982). The hydrogen deficiency of coal ensures the survival of early formed radicals throughout the coalification process (Retcofsky et al. 1968; Levine et al. 1982). The concentration of radicals varies with coal rank, increasing as a function of rank advance and the concomitant expulsion of hydrogen, reflecting the pronounced alteration expected of mature coals (Retcofsky et al. 1968; Kwan and Yen 1979; Krevelen 1993; Więckowski et al. 2000; Qiu et al. 2007). The aromatization of the coal macromolecule is suggested to be related to radical preservation (Austen et al. 1966; Kwan and Yen 1979). The maceral constituents of coal have been found to have varying radical contents (Austen et al. 1966; Grandy and Petrakis 1979; Silbernagel et al. 1984a, b, 1986; Krevelen 1993, and references therein; Więckowski et al. 2000). At the bituminous rank, inertinite group macerals generally have a higher radical content than vitrinite and liptinite counterparts.

Austen et al. (1966) offer three possibilities for the origin of radicals in coal. Firstly, stable radicals are associated with the original organic matter and survive coalification. The radicals form as a result of enzymatic reactions, as well as the oxidation of organic matter during diagenesis. However, since radicals in the initial organic matter would mostly be localized on oxygen atoms, which are progressively expelled during coalification, it is unlikely that these are present in coal of bituminous rank (Austen et al. 1966). Indeed, with an increase in maturity from lignite to bituminous coal, the proportion of radicals localized on oxygen atoms is decreased (Austen et al. 1966). Radicals in such coals may instead be associated

with carbon atoms, as molecular products of reactions related to oxygen expulsion (Austen et al. 1966). Secondly, the radicals form due to an increase in temperature during coalification (Austen et al. 1966; Qiu et al. 2007). The decomposition of methyl and methoxyl, hydroxyl, and carboxyl functional groups through homolytic fission with methane, water, and carbon dioxide as products respectively, results in the formation of radical species. The radicals are subsequently immobilized by the coal structure (Austen et al. 1966; Retcofsky et al. 1968). As the aromatic structure grows with increasing rank, bond breakage is also enhanced and the stable structure required to accommodate and shield the radicals is progressively established. The final mechanism proposed by Austen et al. (1966) is also related to a temperature rise. Radioactive decay of elements within mineral constituents of coal provides the heat required for the breaking of bonds in the organic fraction, resulting in the formation of radicals (Austen et al. 1966). All these three radical-generating processes, so far as they are related to homolytic bond fission during coalification, have subsequently been supported by others (e.g., Retcofsky et al. 1968; Kwan and Yen 1979; Krevelen 1993).

Variations in the radical content of iso-rank macerals are indicative of differences in the degree of thermal alteration of the botanical precursors, thus suggesting differences in origin pathways. The typically high radical content of inertinite macerals suggests pre-diagenesis metamorphism of the botanical precursor (Austen et al. 1966; Retcofsky et al. 1968; Silbernagel et al. 1984a, b, 1986; Więckowski et al. 2000). There are numerous studies on the ESR properties of coal and constituent macerals in the published literature. However, these studies generally address vitrinite-rich northern hemisphere coals (Austen et al. 1966; Retcofsky et al. 1968, 1981; Silbernagel et al. 1984a, b, 1986; Kwan and Yen 1979; Fowler et al. 1987; Więckowski et al. 2000; Qiu et al. 2007; Liu et al. 2014; Zhou et al. 2017), which have been shown to be both compositionally and genetically distinct from southern hemisphere counterparts (Plumstead 1961; Falcon 1986a; Cairncross and Cadle 1988; Falcon and Ham 1988; Hagelskamp and Snyman 1988; Snyman 1989; Cairncross et al. 1990; Taylor et al. 1998; Van Niekerk et al. 2008; O'Keefe et al. 2013). The main consequence of this is a somewhat skewed focus on vitrinite macerals and vitrinite-rich coals, and the results may not be applicable to inertinite-rich South African coals of the Main Karoo Basin.

The present study employs ESR and the fraction of aromaticity inferred from the H/C atomic ratio in the characterization of a parent coal from the No. 4 Seam Upper, Witbank Coalfield, situated in the Main Karoo Basin of South Africa. A vitrinite-rich and an inertinite-rich sample were prepared through density-fractionation. The ESR properties for the three samples are discussed in

conjunction with other coal parameters, including detailed petrographic analysis. The results are used to test whether a fire-origin hypothesis holds for the dominant inertinite macerals present in the coal samples. A fire-origin was proposed for the macerals based on the carbon-13 cross-polarization magic-angle-spinning solid-state nuclear magnetic resonance (^{13}C CP-MAS SS NMR) structural parameters (Moroeng et al. 2018). A similar conclusion was reached in a submitted research article based on stable nitrogen and carbon (δ^{15}N and δ^{13}C) isotopes (Moroeng et al. under review).

2 Materials and methods

2.1 Sample, preparation, and basic characterization

A medium rank C bituminous coal sample from the No. 4 Seam Upper of the Witbank Coalfield was obtained from an operating coal mine. The entire sample ($\sim$ 50 kg) was crushed and screened to between $-$ 2 and $-$ 0.5 mm. A quarter of the material was set aside to represent what is herein referred to as the "parent sample". The remaining material ($\sim$ 17 kg) was subjected to float-sink density separation following South African National Standard (SANS) 7936 (2010) to create a vitrinite-rich (RD = 1.3) and inertinite-rich (R = 1.8) products. A rotary splitter was used to homogenously split each sample into amounts appropriate for the different analyses. These include: proximate, elemental, gross calorific value (CV), petrographic, ESR, δ^{15}N and δ^{13}C values, and ^{13}C CP-MAS SS NMR analysis. For the present study, only the ESR results are reported.

The samples were prepared for petrographic analysis as polished blocks following SANS standard 7404-2 (2015), and the macerals qualified and quantified following SANS standard 7404-3 (2016) using a Zeiss AxioImager M2M reflected-light microscope retrofitted with Hilgers Diskus Fossil components and software, at a total magnification of 500 $\times$ using immersion oil. The mean random vitrinite reflectance (%RoVmr) was determined following SANS 7404-5 (2016). The maceral nomenclature adopted follows that of the International Committee for Coal and Organic Petrology for bituminous coals (ICCP 1998, 2001; Pickel et al. 2017). Proximate, elemental, and CV analyses were performed at a commercial laboratory (Bureau Veritas, Centurion, South Africa) following prescribed SANS standards; SANS 17247 (2006), SANS 17246 (2011), SANS 334 (1992), and SANS 1928 (2009), respectively.

2.2 Electron spin resonance analysis

The ESR analyses were undertaken using a Bruker ESP300E continuous wave X-band ESR spectrometer at ambient temperature ($\sim$ 23 °C). For each coal sample, the following parameters were determined: ESR spectrum, linewidths as a function of microwave power, and the area under the absorption spectrum as a function of microwave power. The variation of the spectrum area as a function of microwave power was fitted to a power law, as described later, and the exponents of the power law extracted.

For each coal sample, a representative (prepared using a rotary splitter) sub-sample was prepared for the ESR analysis. The ESR experiments were conducted on material with particle sizes between $-$ 2 and $-$ 0.5 mm. Milling and demineralization of the samples were considered unnecessary. Fine milling may result in the formation of radicals through bond cleavage as demonstrated by Liu et al. (2014). Although the presence of inorganic matter in coal may affect the resulting ESR spectra, acid-based demineralization may also lead to the loss of oxygenated radicals. Furthermore, the resonance peaks of metal ions are far removed from that of corresponding organic matter (Binet et al. 2002; Qiu et al. 2007). In addition, the ESR spectra of coal samples with varying amounts of mineral matter has also been found to be comparable (Retcosfky et al. 1981; Silbernagel et al. 1986; Qiu et al. 2007, and references therein).

3 Results

3.1 Basic characterization and aromaticity inferred from H/C atomic ratio

The proximate and elemental analyses of the parent coal and the density-fractionated samples are presented in Tables 1 and 2. The H/C atomic ratio was used estimate the aromatic fraction for bituminous rank coals (Maroto-Valer et al. 1994, 1998a; Mazumdar 1999; Van Niekerk et al. 2008; Moroeng et al. 2017), and is applicable for density-fractionated samples (Maroto-Valer et al. 1998b; Davidson 2004). Based on this, the inertinite-rich sample (H/C = 0.74) has the higher aromatic fraction compared to the vitrinite-rich counterpart (H/C = 0.85). The lower volatile content (VM = 28.5 wt%) for the inertinite-rich sample is consistent with the higher aromatic fraction (Van Niekerk et al. 2008, and references therein), as inferred from the H/C ratio. For the inertinite-rich sample, the H/C atomic ratio is within the range (0.51 < H/C < 0.75) previously reported by Maroto-Valer et al. (1998b) for various inertinite-rich coals at the bituminous range of rank.

Table 1 Proximate analysis and calorific value (CV) (air dried) of the parent, inertinite-rich, and vitrinite-rich samples

Sample	Proximate analysis (wt%)				Gross calorific value (MJ/kg)
	Moisture	Ash	Volatile matter	Fixed carbon	
Parent	3.10	12.50	30.70	53.70	27.69
Inertinite-rich	3.00	13.40	28.50	55.10	27.14
Vitrinite-rich	3.10	4.20	38.60	54.10	30.91

Table 2 Elemental analyses (air dried) for the parent, inertinite-rich, and vitrinite-rich samples

Sample	Elemental analysis (wt%)					H/C
	C	H	N	O	S	
Parent	67.40	4.40	1.80	8.61	2.24	0.78
Inertinite-rich	67.60	4.17	1.68	9.57	0.64	0.74
Vitrinite-rich	75.00	5.33	2.07	9.58	0.76	0.85

Maceral group compositions for the parent, inertinite-rich, and vitrinite-rich samples are presented in Fig. 1, and the detailed maceral composition is given in Table 3. The sample is a medium rank C bituminous coal (0.65 %oVmr) as determined on the parent sample. The principal vitrinite macerals are collodetrinite and collotelinite with subordinate amounts of corpogelinite. As may be expected, the proportion of these macerals is greatest in the vitrinite-rich sample. Semifusinite constitutes a significant proportion of both the parent and inertinite-rich samples at approximately 18 vol% and 29 vol%, respectively. In contrast, this maceral constitutes 5 vol% of the vitrinite-rich sample.

Inertodetrinite is the second most abundant inertinite maceral at 24 vol% in the inertinite-rich sample and 20 vol% in the parent sample. The fusinite content is similar for the parent and inertinite-rich samples at approximately 8 vol%, and 4 vol. for the vitrinite-rich sample. The petrographic composition of the inertinite-rich sample is consistent with the higher fraction of aromaticity relative to the vitrinite-rich counterpart, as inferred from the H/C atomic ratio and in agreement with the findings by Van Niekerk et al. (2008).

3.2 Electron spin resonance: spectral amplitudes, line-shapes, and line-widths

For each sample, measurements of the ESR spectrum were taken at a microwave power of approximately 2.6 mW, where 10 sweeps were taken to improve the signal-to-noise ratio. An attempt was made to fit the experimental data, the derivative of the absorption curve, to Gaussian and Lorentzian distributions; the latter is by far the best fit for all three samples (Fig. 2). A Gaussian distribution is typically observed in low rank coals with higher rank coals (> 90% carbon) exhibiting a Lorentzian spectra line-shape
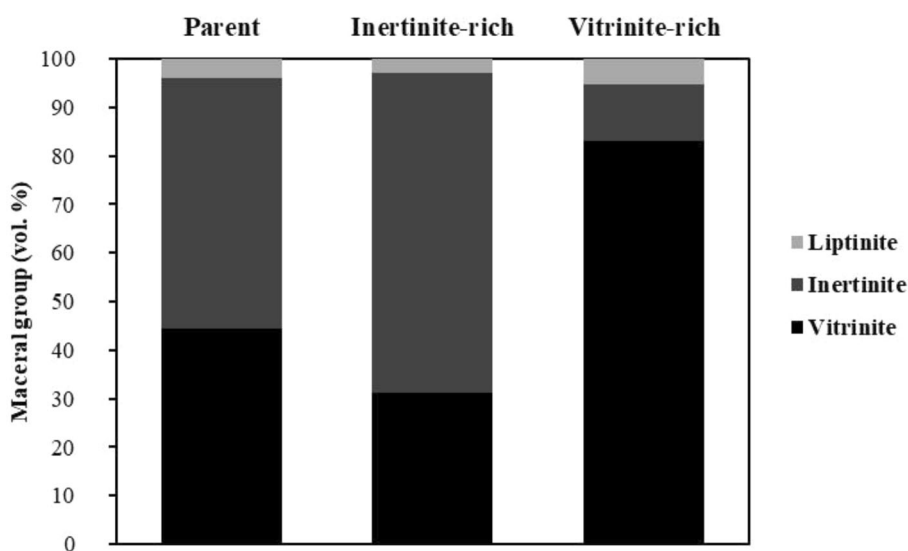
Fig. 1 Distribution of maceral groups (mineral-matter-free basis) for the parent, inertinite-rich and vitrinite-rich samples

Table 3 Maceral composition (vol%) for the parent, inertinite-rich, and vitrinite-rich samples

	Parent	Inertinite-rich	Vitrinite-rich
Telinite	0.2	0.0	2.4
Collotelinite	12.0	12.4	35.3
Vitrodetrinite	0.0	0.0	0.0
Collodetrinite	28.0	15.4	36.3
Corpogelinite	1.4	0.5	6.9
Gelinite	0.0	1.3	0.0
Pseudovitrinite	0.0	0.2	0.4
Total vitrinite	**41.6**	**29.8**	**81.3**
Fusinite	8.6	8.3	3.9
Semifusinite	18.3	28.9	4.7
Micrinite	0.4	0.2	0.0
Macrinite	0.2	0.2	0.4
Secretinite	1.2	1.2	0.6
Funginite	0.0	0.0	0.0
Inertodetrinite	19.8	23.8	1.8
Total inertinite	**48.5**	**62.6**	**11.4**
Sporinite	3.3	2.9	2.9
Cutinite	0.4	0.0	2.0
Resinite	0.0	0.0	0.2
Alginite	0.0	0.0	0.0
Liptodetrinite	0.0	0.0	0.0
Exsudatinite	0.0	0.0	0.0
Total liptinite	**3.7**	**2.9**	**5.1**
Silicate	3.1	3.1	0.2
Sulphide	2.4	1.2	0.8
Carbonate	0.8	0.6	1.4
Total minerals	**6.3**	**4.9**	**2.4**
%RoVmr	**0.65**		
Std. Dev.	**0.067**		

Bold indicates the totals for the different maceral components

%RoVmr, mean random vitrinite reflectance

(Retcofsky et al. 1968). However, in the present case, the highest carbon content is only 75% for the vitrinite-rich sample. A Lorentzian distribution suggests a random distribution of radicals with the shape and associated linewidth resulting from dipole–dipole interactions (Silbernagel et al. 1984b).

The presence of a single peak in the spectra for the parent, inertinite-rich, and vitrinite-rich samples is due to the presence of radicals in the organic fraction of the coals. Furthermore, a single well-defined peak suggests the absence of radicals in the inorganic fraction (Binet et al. 2002). However, there are some notable differences between the spectral distributions for the three samples. Firstly, the spectrum peak for the inertinite-rich sample is markedly narrower than the other two samples with the vitrinite-rich sample exhibiting the broadest peak (Fig. 2).
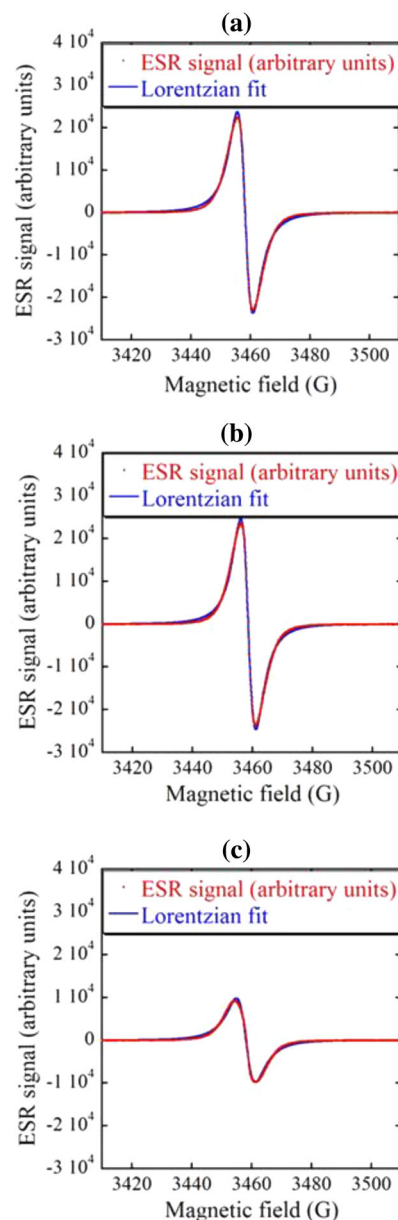
Fig. 2 ESR spectra for **a** the parent, **b** inertinite-rich, and **c** vitrinite-rich coal samples

In addition, the peak amplitudes appear roughly the same for both the parent and inertinite-rich samples. This is indicative of the intensity of the ESR signal and is proportional to the number of radicals in the samples. The vitrinite-rich sample has a much lower peak, indicative of a much lower radical content. Furthermore, the Lorentzian fit is evidently poorer for this sample in addition to the experimental spectrum showing slight asymmetry. Conversely, the spectra are largely symmetric and more pronounced for the inertinite-rich sample and, to a slightly lesser extent, the parent coal.

Measurements of the linewidth as a function of microwave power (Fig. 3) were taken in the 0.80–280 mW range in steps of 2 dB. The behaviour of the parent coal is similar to that exhibited by the inertinite-rich sample. The behaviour of the vitrinite-rich sample is altogether different. At a microwave power of 1 mW, the linewidths for both the parent and inertinite-rich samples are roughly 4.4 Gauss (G). The corresponding linewidth for the vitrinite-rich sample is markedly higher at approximately 5.5 G. The linewidth for the vitrinite-rich sample then decreases with increasing power, reaching a minimum of $\sim$ 5.1 G at around 100 mW. The decrease in the corresponding
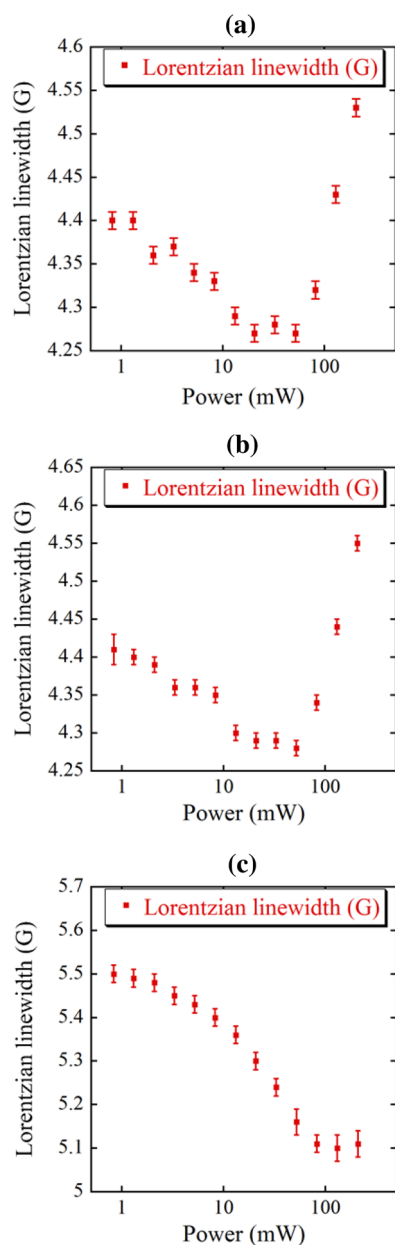
Fig. 3 Lorentzian linewidth as a function of microwave power for **a** the parent, **b** inertinite-rich, and **c** vitrinite-rich coal samples

linewidths for the other two samples are less pronounced, only reaching a minimum at a power of $\sim$ 80 mW then rising again more rapidly. Linewidths for the vitrinite-rich sample as a function of increasing microwave power are consistently higher than those for both the parent and inertinite-rich samples. It must be noted that the minimum linewidth for the inertinite-rich sample at a power just below 100 mW is lower for the parent sample. The linewidth for low rank coals with a carbon content of less than 90% is reported to be within the range 5.9–8.0 G (Retcofsky et al. 1968). This appears to be higher than the values obtained for the samples of the present study. It has also been shown that the variation in width is not due to the presence of radical species with varying g-values and is, thus, not due to radicals localized on different host molecules or atoms (Retcofsky et al. 1968).

The area under the absorption curve (integral of the derivative spectra obtained) for each sample was similarly measured as a function of microwave power (Fig. 4). Each derivative spectrum was integrated numerically to obtain the absorption curve, and the area under the curve was determined numerically. This produces a result that is proportional to the number of unpaired electrons in each sample. The peak amplitude was determined from a double integral of the experimentally obtained derivative for each microwave power. Amplitude is plotted as a function of microwave power for each sample in Fig. 4. The data were subsequently fitted using a regression power law of the form:

$$A = A_0 P^n \tag{1}$$

where A is the amplitude of the ESR signal; P is the microwave power; and A_0 and n are obtained from fitting the data.

In a case where a saturation peak is not observed, and the resonance line is homogeneously broadened, we expect $n \approx 0.5$. The resulting exponents for each sample are provided in the caption to Fig. 4. The exponents for the parent and inertinite-rich samples are comparable at 0.68 and 0.65, respectively. As such, the parent and inertinite-rich samples have similar radical contents, with similar relaxation times. However, the slight broadening of the spectral line-shape for the parent sample suggests small differences in the radical properties of the two samples. The power law exponent for the vitrinite-rich sample is significantly lower, and suggests that the radical concentration is lower than for the other two samples, and that the radicals may be in a different chemical environment. This observation is in agreement with previous studies (e.g., Austen et al. 1966; Retcofsky et al. 1968; Silbernagel et al. 1984a, b, 1986). The parent and inertinite-rich samples thus exhibit similar behaviour as is the case with both the spectra line-shape and width. None of the three samples

(a)

(b)

(c)
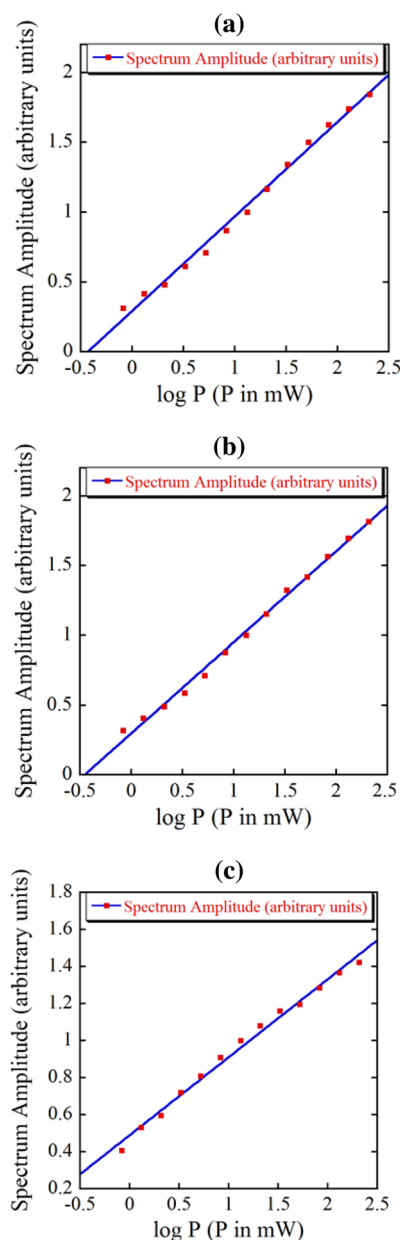
Fig. 4 Spectrum amplitude as a function of microwave power for **a** the parent, **b** inertinite-rich, and **c** vitrinite-rich samples. The exponents for each of the power law fits are **a** 0.68 ± 0.02, **b** 0.65 ± 0.01, and **c** 0.42 ± 0.01

showed a saturation peak over the power range explored. This suggests that the spin–lattice relaxation rate is high for all three samples at room temperature (~ 23 °C), i.e. T_1 is small. The difference in the exponents obtained for the parent and inertinite-rich samples on one hand, and the vitrinite-rich sample on the other, suggest that the spectral lines may originate from different environments. It would be of interest to perform saturation measurements at low temperatures, where the relaxation rate is lower, as this may uncover unresolved fine structure in the ESR spectra.

4 Discussion

4.1 Radical properties for vitrinite-rich and inertinite-rich Witbank coals

Based on the petrographic composition and elemental analysis including the H/C atomic ratio, the parent sample is most comparable to the inertinite-rich sample. The ESR properties are largely consistent with this observation. The high collotelinite and collodetrinite content of the vitrinite-rich sample appears to be responsible for the deviation from a pure Lorentzian fit, resulting in a lower peak amplitude and slightly asymmetric distribution. Peak narrowing of a Lorentzian distribution, as observed in the line-shape of the inertinite-rich sample, is interpreted to reflect pronounced radical mobility, i.e., the migration of radical electrons between neighbouring molecular hosts (Retcofsky et al. 1968; Kwan and Yen 1979; Silbernagel et al. 1984a, b, 1986). In addition, exchange interactions between neighbouring radicals can also effect narrowing of the spectrum peak (Silbernagel et al. 1984b; Kwan and Yen 1979). The former phenomenon inevitably requires that the individual host molecules be relatively close to each other, whereas the latter necessitates a high spin density. The peak narrowing exhibited by the line-shape for the inertinite-rich sample suggests an increase in either or both radical motion and exchange interactions.

The greater aromatic fraction of both the inertinite-rich and parent samples is consistent with the likelihood of pronounced radical migration. With increasing aromaticity, the merging and condensation of aromatic rings (Solum et al. 1989; Haenel 1992; Davidson 2004; Suggate and Dickinson 2004; Van Niekerk et al. 2008; Chen et al. 2012) implies that a molecular host becomes progressively larger (Kwan and Yen 1979). Spatially, greater aromaticity suggests that the area over which a radical electron is able to move is therefore also enlarged. In addition, the reduction in distance between adjacent molecules (Van Niekerk et al. 2008) implies that a radical electron is better able to interchange hosts. Larger aromatic cluster sizes as well as the greater degree of condensation associated with higher aromaticity are thus consistent with prominent radical mobility (Kwan and Yen 1979; Więckowski et al. 2000). The higher spin densities for the parent and inertinite-rich samples, coupled with greater aromaticity, permits greater exchange interactions between adjacent radical species. Owing to greater aromatic fraction, radicals in the inertinite-rich sample may be associated with larger aromatic molecular hosts (Fig. 5) (Van Niekerk et al. 2008).

The considerably broader and less than perfect spectrum fit for the vitrinite-rich sample, coupled with lower aromaticity, is attributable to reduced radical migration and
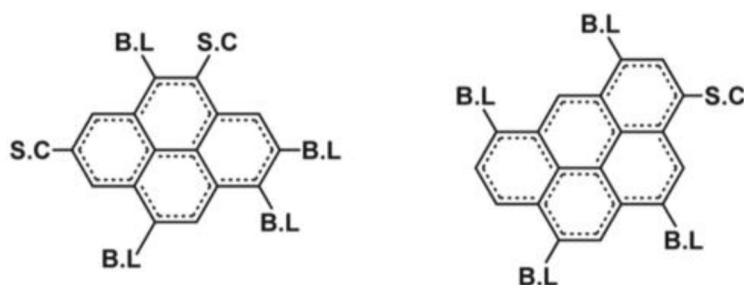
Fig. 5 Representations of the average molecular host size and attachments for vitrinite-rich Waterberg and inertinite-rich Highveld coal. S.C., side chains, B.L. bridges and loops (Van Niekerk et al. 2008)

exchange interactions. According to Silbernagel et al. (1986), individual molecular hosts should, in this case, be viewed as somewhat isolated from one another. As a result of lower aromaticity, the cluster sizes are presumably smaller in comparison to those found in the inertinite-rich counterpart (Van Niekerk et al. 2008). Van Niekerk et al. (2008) also found that for bituminous coals of comparable rank, the interplanar distances determined using X-ray diffraction (XRD) were 3.97Å for vitrinite-rich Waterberg and 3.42Å for inertinite-rich Highveld coals. The reduced interplanar distance along with larger cluster sizes for the more aromatic inertinite-rich Highveld sample (Fig. 5) is a reflection of a more condensed molecular structure. This would, in turn, result in resonance stabilization leading to relatively unreactive and stable radicals (Austen et al. 1958). Therefore, with a narrowed ESR peak, the aromatic clusters and other molecules which serve as radical hosts are closer to one another. This implies that radical mobility is enhanced in a greater aromatic fraction coal. It should be mentioned that Moroeng et al. (2018) report the average aromatic cluster size for the inertinite-rich sample (determined using ^{13}C CP-MAS SS NMR) to be comprised of six-aromatic carbons (a single aromatic ring), implying a reduction in resonance stabilization for the radicals of this sample.

Conversely, in a sample with a broadened peak, the hosts are further apart, thus impeding radical motion resulting in the restriction of a radical electron to a single host. This coupled with a lower spin density is consistent with a reduction in exchange interactions due to the larger distance between molecular hosts and, consequently, radical electrons. With smaller hosts, with less a condensed molecular structure, resonance stabilization is diminished resulting in more reactive radical species (Austen et al. 1958). Notwithstanding lower aromaticity and spin density, radical motions and exchange interactions are present, albeit minimized, in the vitrinite-rich sample. Given that rank-dependent variations can be completely excluded (samples created from the same coal), the observed differences are attributable only to variations amongst the

dominant macerals present in the density-fractionated samples.

Radical motions and exchange interactions are thus greatest in the inertinite-rich sample. These phenomena appear to decrease as a function of aromaticity and evidently, inertinite content in the order: inertinite-rich sample > parent sample > vitrinite-rich sample. In particular, radical mobility and exchange interactions appear to be greatest in a Witbank coal dominated by fusinite, semi-fusinite, and inertodetrinite; and reduced in a sample with a greater proportion of collotelinite and collodetrinite. These observations are consistent with the widely accepted view that the compositional differences between inertinite and vitrinite macerals derive mainly from genetic, depositional environment-specific variations. Metamorphosis of inertinite-forming precursors before diagenesis and/or incorporation into a peat-forming environment has been suggested by Austen et al. (1966) and Silbernagel et al. (1984b).

4.2 On the formation of the inertinite macerals in the Witbank Coalfield

Vitrinite-rich and inertinite-rich samples derived from the same coal have lower and higher radical contents, respectively. This suggests independent origin pathways for the dominant macerals present in each coal sample. Differences in the pathways must have occurred before the precursors for the dominant macerals of each density-fractionated sample underwent diagenesis in a classic peat-forming environment, wherein geochemical coalification, affecting the sum total of coal-forming materials, took place. Any other process affecting the materials during coalification should have imparted similar characteristics on all coal-forming materials. The dominant macerals of vitrinite-rich sample, collotelinite and collodetrinite, formed through humification and gelification of woody tissues in a water-logged setting (Teichmüller 1989; Diessel 1992; Krevelen 1993; ICCP 1998; Taylor et al. 1998; Hower et al. 2013; O'Keefe et al. 2013). Vitrinite

formation is thus consistent with the lower radical content for the vitrinite-rich sample, thus lacking the pronounced, heat-induced alteration associated with fusinite genesis.

The high inertinite content in the coals of the Main Karoo Basin of South Africa, has historically been attributed to aerial oxidation and incomplete degradation of plant matter as a result of a cold climate (Falcon 1986a, 1989; Hagelskamp and Snyman 1988; Snyman 1989; Cadle et al. 1993; Van Niekerk et al. 2008; O'Keefe et al. 2013). At the same time, others contend that the inertinite component of the coals of the Main Karoo Basin is a product of charring of plant matter (Glasspool 2003a, b; Jasper et al. 2013; Moroeng et al. 2018). Given the complexity associated with coal formation, and consequent chemical and physical characteristics, it seems unlikely that inertinite genesis was the same in all the coal-forming regions of the world, or even, within a singular peat-forming environment (Austen et al. 1966; Diessel 1992; Moore et al. 1996; Moore and Shearer 1997; Taylor et al. 1998; ICCP 2001; Hower et al. 2011b; Richardson et al. 2012; Jasper et al. 2013), what some commonly refer to as multiple origin pathways (Hower et al. 2011a, 2013; O'Keefe and Hower 2011; O'Keefe et al. 2013; Moroeng et al. 2018).

Austen et al. (1966) report high radical contents for fusinite-rich coals relative to fusinite-impoverished counterparts, and found that the spin density of the former coals did not change during pyrolysis experiments at temperatures below 550 °C. As a result, Austen et al. (1966, p. 357) concluded that "fusinites achieved both their carbon contents and their high unpaired spin concentration before incorporation into the sediment and most probably by exposure to elevated temperatures". The relatively high temperatures required for inertinite formation can be provided by peat- or wildfires, or alternatively, by thermophilic bacteria and/or fungal activity (Austen et al. 1966; Scott 1989, 2002, 2010; Diessel 1992; Moore et al. 1996; Moore and Shearer 1997; Glasspool 2003a, b; Scott and Glasspool 2007; Hower et al. 2011a, b, 2013; Richardson et al. 2012; Jasper et al. 2013; O'Keefe et al. 2013; Moroeng et al. 2018). However, when organisms degrade plant matter, anatomical structure is destroyed (Guo and Bustin 1998; Hower et al. 2011a, b, 2013; Richardson et al. 2012; O'Keefe et al. 2013). Furthermore, macerals produced through fungal activity possess indistinct cell walls (Taylor et al. 1998), and fungal hyphae length has been observed to correlate with the fusinitized sections of a plant organ (Moore et al. 1996; Moore and Shearer 1997). In contrast, wood charring produces anatomical structures similar to those observed in certain inertinite macerals (Scott 1989, 2002, 2010; Teichmüller 1989; Jones and Chaloner 1991; Guo and Bustin 1998; Scott and Glasspool 2007; Ascough et al. 2010), noted by

Moroeng et al. (2018) for the inertinite macerals of the coal samples of the present study. If the same line of reasoning applied by Austen et al. (1966) with regards to fusinite genesis is applied to the dominant inertinite macerals of the inertinite-rich sample, the high radical content of this sample can be interpreted to suggest that the major components were subjected to thermally driven pre-diagenesis metamorphism.

Fusinite and semifusinite macerals present in the inertinite-rich Witbank coal sample of this study likely represent charred plant matter. The preservation of anatomical structure and reflectance of semifusinite, coupled with the higher radical content for the inertinite-rich sample, suggest charring of botanical precursor, albeit to a lesser degree than corresponding fusinite within the same coal sample. In this sense, a fusinite-rich section of a coal particle may be interpreted to represent the outermost layers of a plant organ. The inner, comparatively lower-reflectance portions of the same particle may then represent semifusinite. During charring, the outermost layers of a plant organ would have been directly exposed to the fire, whereas the inner portions would have been shielded and may thus, have remained relatively unaffected by the elevated temperature (Scott 2010). This process accounts for a gradational boundary between fusinite and adjacent semifusinite, as shown in Figs. 6 and 7. In the absence of a gradational contact between inertinite macerals as shown in Fig. 8, the botanical organs can be interpreted to have been distinct and discrete. However, fusinite and semifusinite would still have formed from woody plant organs. The degree of charring, controlled in part, by moisture and perhaps size of the affected plant organ, would then have determined whether fusinite or semifusinite was formed.

A fusinite particle of uniformly high reflectance (Fig. 9) may be interpreted to reflect charring when the botanical precursor had already died and was dried out, and was thus, more readily and evenly charred. The preservation of anatomical structure suggests negligible degradation by organisms (Guo and Bustin 1998; Richardson et al. 2012; Hower et al. 2013; O'Keefe et al. 2013), and thus the plant matter in question must have been located either at the top, above the water level, or outside the peat-forming environment before charring. Following this line of reasoning, the formation of semifusinite may represent charring while plant matter was still wet, potentially alive or recently deceased, with the increased moisture content hindering both complete charring and the attainment of very high reflectances. According to Jasper et al. (2013), the increased atmospheric oxygen content during the Permian Period would have rendered wet vegetation more flammable. In this sense, the relatively high semifusinite content of the coals of the Main Karoo Basin likely represents coal-forming environments wherein incomplete/partial
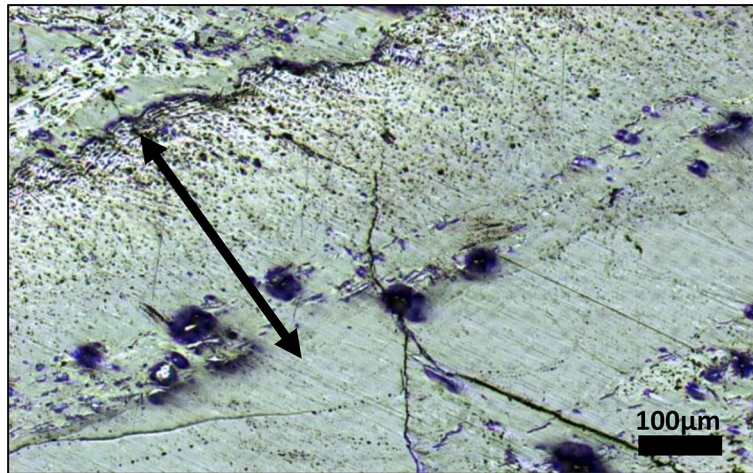
Fig. 6 Fusinite grading into semifusinite and, finally into vitrinite, observed in the inertinite-rich sample. × 100 magnification, reflected light in air (photomicrograph, H. Dorland). Scale is indicated

Fig. 7 Mosaic photomicrograph showing fusinite (right; well-preserved structure, high reflectance) grading into semifusinite (structured still, lower reflectance), and finally into vitrinite (bottom left; unstructured, lowest reflectance) observed in the inertinite-rich sample. × 500 magnification, reflected light under oil immersion. Scale is indicated
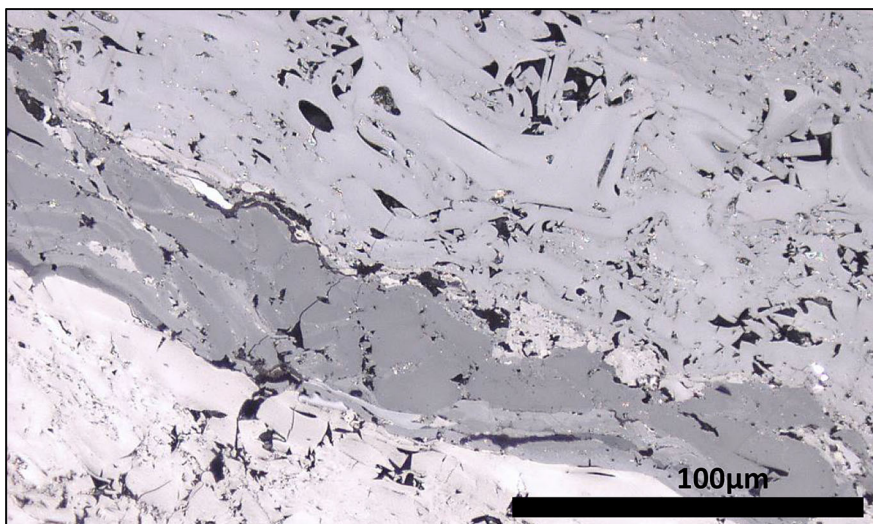
Fig. 8 Inertinite macerals with varying reflectances observed in the inertinite-rich sample. × 500 magnification, reflected light with oil immersion. Scale is indicated
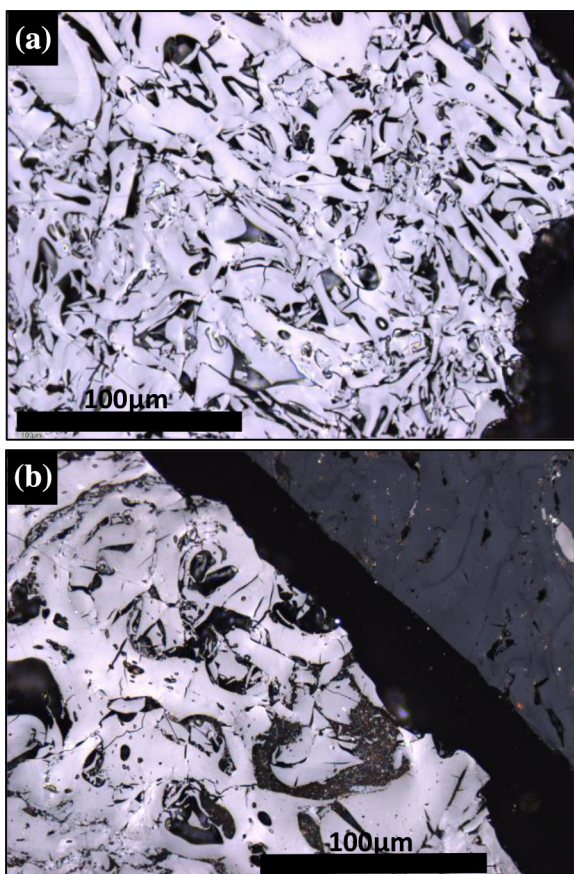
Fig. 9 **a**, **b** Fusinites observed in the inertinite-rich sample. × 500 magnification, reflected light with oil immersion. Scale is indicated

Fig. 10 **a** Alternating layers of inertodetrinite and vitrinite; **b** inertodetrinite, observed in the inertinite-rich sample. × 500 magnification, reflected light with oil immersion. Scale is indicated

charring was prevalent. Charred and disintegrated plant matter could have resulted in smaller fragments blown into, or transported into the peat-forming environment through some other sedimentary process, resulting in the formation of inertodetrinite (Fig. 10).

Glasspool (2003b) notes the inherent contradiction required to reconcile the water-logged environments generally required for peat accumulation alongside the relatively dry conditions required for the formation of fire-derived inertinite macerals, and thus account for the high radical content of the inertinite-rich sample of this study. This is attributed to an interchange between periods of pronounced saturation and relatively drier periods (Glasspool 2003b). Similar conditions, specifically the changes in climatic conditions are also invoked in the present case and appear to be particularly applicable given the general alternation of bright and dull coloured banding present in the coals, broadly corresponding to vitrinite-rich and inertinite-rich bands (Falcon 1989). The dry periods could thus coincide with periods of pronounced wild- and peat-fire events (Hope et al. 2005), resulting in the formation of a significant amount of fire-derived inertinite macerals, with the wetter periods giving rise to mostly vitrinite

macerals. Gondwana climatic conditions are generally interpreted to have been varied, ranging from cold to cool, and dry to wet (Falcon 1986a; Cairncross 1990, 2001; Cadle et al. 1993). However, more recent studies have shown that the climate was warming during the formation of the younger coal seams of the Main Karoo Basin (Ruckwied et al. 2014). Furthermore, the occurrence of fires, i.e., the proposed pathway for the formation of the dominant inertinite macerals, within and around Gondwana peat-forming environments, including in South Africa, has been established based on the presence of fossilized charcoal (e.g., Glasspool 2003a, b; Jasper et al. 2013; Slater et al. 2015).

5 Conclusion

For the first time, ESR was used to characterize an inertinite-rich and a vitrinite-rich sample of the same coal from the No. 4 Seam Upper, Witbank Coalfield (South Africa). In addition, the H/C atomic ratio was used to infer the fraction of aromaticity. The medium rank C bituminous

parent coal sample density-fractionated. Semifusinite and inertodetrinite were the dominant macerals of the inertinite-rich sample (62.6% total inertinite), whereas the vitrinite-rich sample (81.3% total vitrinite) was dominated by collotelinite and collodetrinite. The radical (unpaired electrons) content as determined by ESR is highest in the inertinite-rich sample, followed by the parent sample, with the vitrinite-rich sample having the lowest radical content. The H/C ratios suggest that the fraction of aromaticity follows the same trend, with the inertinite-rich and vitrinite-rich samples having a higher and lower aromatic fraction, respectively. The ESR properties were used to examine the sustainability of a fire-origin for the dominant inertinite macerals. The main findings of the study can be summarized as follows:

(1) In addition to having the higher radical content, the inertinite-rich sample also has a narrowed ESR spectrum peak. This reflects radical mobility and exchange interactions between adjacent radicals. The higher aromatic fraction of this sample suggests proximity of radicals, and that the radicals interchange between molecular hosts.

(2) Owing to a higher radical concentration in the inertinite-rich sample, the dominant inertinite macerals of this coal sample are suggested to have formed in a similar manner as is widely accepted for fusinite, i.e., through charring of botanical precursors.

(3) It is argued that a coal particle—comprised of fusinite grading into semifusinite—reflects differences in degrees of charring for these macerals, controlled by the inherent moisture content and size of the botanical organ. Thus, semifusinite formation reflects moderate charring, whereas fusinite is indicative of near complete charring.

(4) Based on the degree of charring, and given a sufficiently thick plant organ, an individual organ may form both macerals with a gradational contact separating the two. In the case where the contact is sharp, the two macerals have been formed from individual plant organs that were subsequently superimposed.

(5) Inertodetrinite represents charred/partially charred plant matter that was subsequently fragmented.

Compliance with ethical standards

References

Ascough PL, Bird MI, Scott AC, Collinson ME, Cohen-Ofri I, Snape CE, Le Manquais K (2010) Charcoal reflectance measurements: implications for structural characterization and assessment of diagenetic alteration. J Archaeol Sci 37:1590–1599

Austen DEG, Ingram DJE, Tapley JG (1958) The investigation of free radicals trapped in low temperature carbons. Trans Faraday Soc 54:400–408

Austen DEG, Ingram DJE, Given PH, Binder CR, Hill LW (1966) Electron spin resonance study of pure macerals. In: Given PH (ed) Coal science, advances in chemistry, vol 55. American Chemical Society, Washington, DC, pp 344–362

Binet L, Gourier D, Derenne S, Robert F (2002) Heterogeneous distribution of paramagnetic radicals in the insoluble organic matter from the Orgueil and Murchison meteorites. Geochim Cosmochim Acta 66(23):4177–4186

Cadle AB, Cairncross B, Christie ADM, Roberts DL (1993) The Karoo Basin of South Africa: type basin for coal-bearing deposits of southern Africa. Int J Coal Geol 23:117–157

Cairncross B (1990) Tectono-sedimentary settings and controls of the Karoo Basin Permian coals, South Africa. Int J Coal Geol 16(1–3):175–178

Cairncross B (2001) An overview of the Permian (Karoo) coal deposits of Southern Africa. J of Afr Earth Sci 33:529–562

Cairncross B, Cadle AB (1988) Palaeoenvironmental control on coal formation, distribution and quality in the Permian Vryheid Formation, East Witbank Coalfield, South Africa. Int J Coal Geol 9(4):343–370

Cairncross B, Hart RJ, Wills JP (1990) Geochemistry and sedimentology of coal seams from the Permian Witbank Coalfield, South Africa; a means of identification. Int J Coal Geol 16(4):309–325

Chen Y, Mastalerz M, Schimmelmann A (2012) Characterization of chemical functional groups in macerals across different coal ranks via micro-FTIR spectroscopy. Int J Coal Geol 104:22–33

Davidson RM (2004) Studying the structural chemistry of coal. IEA Clean Coal Centre, p 121

Diessel CFK (1992) Coal-bearing depositional systems. Springer, Berlin, p 721

Dyrkacz GR, Bloomquist CAA, Ruscic L (1984) Chemical variations in coal macerals separated by density gradient centrifugation. Fuel 63:1166–1173

Falcon RM (1986a) Spontaneous combustion of the organic matter in discards from the Witbank coalfield. J South Afr Inst Min Metall 86(7):243–250

Falcon RMS (1986b) A brief review of the origin, formation, and distribution of coal in southern Africa. In: Anhaeusser CR, Maske S (eds) Mineral deposits of Southern Africa, vol I and II. Geological Society of South Africa, Johannesburg, pp 1879–1898

Falcon RMS (1989) Macro-and micro-factors affecting coal-seam quality and distribution in southern Africa with particular reference to the No. 2 seam, Witbank coalfield, South Africa. Int J Coal Geol 12(1–4):681–731

Falcon R, Ham AJ (1988) The characteristics of Southern African coals. J South Afr Inst Min Metall 88(5):145–161

Fowler TG, Bartle KD, Kandiyoti R (1987) Low temperature processes in a bituminous coal studied by in situ electron spin resonance spectroscopy. Fuel 66(10):1407–1412

Glasspool I (2003a) Palaeoecology of selected South African export coals from the Vryheid Formation, with emphasis on the role of heterosporous lycopods and wildfire derived inertinite. Fuel 82:959–970

Glasspool IJ (2003b) Hypautochthonous-allochthonous coal deposition in the Permian, South African, Witbank Basin No. 2 seam; a combined approach using sedimentology, coal petrology and palaeontology. Int J Coal Geol 53:81–135

Grandy DW, Petrakis L (1979) Esr investigation of free radicals in solvent-refined coal materials. Fuel 58:239–240

Guo Y, Bustin RM (1998) FTIR spectroscopy and reflectance of modern charcoals and fungal decayed woods: implications for studies of inertinite in coals. Int J Coal Geol 37:29–53

Haenel MW (1992) Recent progress in coal structure research. Fuel 71:1211–1223

Hagelskamp HHB, Snyman CP (1988) On the origin of low-reflecting inertinites in coals from the Highveld Coalfield, South Africa. Fuel 67:307–313

Hope G, Chokkalingam U, Anwar S (2005) The stratigraphy and fire history of the Kutai Peatlands, Kalimantan, Indonesia. Quatern Res 64:407–417

Hower JC, O'Keefe JMK, Eble CF, Raymond A, Valentim B, Volk TJ, Richardson AR, Satterwhite AB, Hatch RS (2011a) Notes on the origin of inertinite macerals in coal: evidence for fungal and arthropod transformations of degraded macerals. Int J Coal Geol 86(2–3):231–240

Hower JC, O'Keefe JMK, Eble CF, Volk TJ, Richardson AR, Satterwhite AB, Hatch RS, Kostova IJ (2011b) Notes on the origin of inertinite macerals in coals: funginite associations with cutinite and suberinite. Int J Coal Geol 85(1):186–190

Hower JC, Wagner NJ, O'Keefe JMK, Drew JW, Stucker JD, Richardson AR (2012) Maceral types in some Permian southern African coals. Int J Coal Geol 100:93–107

Hower JC, O'Keefe JMK, Wagner NJ, Dai S, Wang X, Xue W (2013) An investigation of Wulantuga coal (Cretaceous, Inner Mongolia) macerals: paleopathology of faunal and fungal invasions into wood and the recognizable clues for their activity. Int J Coal Geol 114:44–53

Ikoma T, Ito O, Tero-Kubota S (2002) Exploring radicals in carbonaceous solids by means of pulsed EPR spectroscopy. Energy Fuels 16:40–47

International Committee for Coal and Organic Petrology (ICCP) (1998) The new vitrinite classification. (ICCP System 1994). Fuel 77(5):349–358

International Committee for Coal and Organic Petrology (ICCP) (2001) The new inertinite classification (ICCP System 1994). Fuel 80(4):459–471

Jasper A, Guerra-Sommer M, Abu Hamad AMB, Bamford M, Cerruti Bernardes-de-Oliveira ME, Tewari R, Uhl D (2013) The burning of Gondwana: Permian fires on the southern continent—a palaeobotanical approach. Gondwana Res 24(1):148–160

Jones TP, Chaloner WG (1991) Fossil charcoal, its recognition and palaeoatmospheric significance. Palaeogeogr Palaeoclimatol Palaeoecol (Global and Planetary Change Section) 97:39–50

Krevelen DW (1993) Coal: typology-physics-chemistry-constitution, 3rd edn. Elsevier, Amsterdam, p 979

Kwan CL, Yen TF (1979) Electron spin resonance study of coal by line width and line shape analysis. Anal Chem 51(8):1225–1229

Levine DG, Schlosber RH, Silbernagel BG (1982) Understanding the chemistry and physics of coal structure (a review). Proc Natl Acad Sci USA 79:3365–3370

Liu J, Jiang X, Shen J, Zhang H (2014) Chemical properties of superfine pulverized coal particles. Part 1. Electron paramagnetic resonance analysis of free radical characteristics. Adv Powder Technol 25(3):916–925

Maroto-Valer MM, Love GD, Snape CE (1994) Relationship between carbon aromaticities and H/C ratios for bituminous coals. Fuel 73(12):1926–1928

Maroto-Valer MM, Andresén JM, Snape CE (1998a) Verification of the linear relationship between carbon aromaticities and H/C ratios for bituminous coals. Fuel 77(7):783–785

Maroto-Valer MM, Taulbee DN, Andresén JM, Hower JC, Snape CE (1998b) Quantitative ^{13}C NMR study of structural variations within the vitrinite and inertinite maceral groups for a semi-fusinite-rich bituminous coal. Fuel 77(8):805–813

Mazumdar BK (1999) On the relationship between carbon aromaticities and H/C ratios for bituminous coals. Fuel 78:1239–1241

Moore TA, Shearer JC (1997) Evidence for aerobic degradation of Palangka Raya Peat and implications for its sustainability. In: Rieley JO, Page SE (eds) Tropical peatlands. Samara Publishing Limited, Cardigan, pp 157–167

Moore TA, Shearer JC, Miller SL (1996) Fungal origin of oxidized plant material in the Palangkaraya peat deposit, Kalimantan Tengah, Indonesia: implications for 'inertinite' formation in coal. Int J Coal Geol 30:1–23

Moroeng OM, Roberts RJ, Bussio JP, Dixon RD (2017) Self-heating potential of coal inferred from elemental data—a case-study of the Witbank Coalfield of South Africa. Energy Fuels 31(11):11811–11817

Moroeng OM, Wagner NJ, Brand DJ, Roberts RJ (2018) A nuclear magnetic resonance study: implications for coal formation in the Witbank Coalfield, South Africa. Int J Coal Geol 188:145–155

Moroeng OM, Wagner NJ, Hall G, Roberts RJ (under review) Using δ^{15}N and δ^{13}C and nitrogen functionalities to support a fire-origin for certain inertinite macerals in a No. 4 Seam Upper Witbank coal, South Africa. Organic Geochemistry

O'Keefe JMK, Hower JC (2011) Revisiting Coos Bay, Oregon: a re-examination of funginite–huminite relationships in Eocene subbituminous coals. Int J Coal Geol 85(1):34–42

O'Keefe JMK, Bechtel A, Christanis K, Dai S, DiMichele WA, Eble CF, Esterle JS, Mastalerz M, Raymond AL, Valentim BV, Wagner NJ, Ward CR, Hower JC (2013) On the fundamental difference between coal rank and coal type. Int J Coal Geol 118:58–87

Petrakis L, Grandy DW (1981) Free radicals in coals and coal conversion. 4. Investigation of the free radicals in selected macerals upon liquefaction. Fuel 60:120–124

Pickel W, Kus J, Flores D, Kalaitzidis S, Christanis K, Cardott BJ, Misz-Kennan M, Rodrigues S, Hentschel A, Hamor-Vido M, Crosdale P, Wagner N, ICCP (2017) Classification of liptinite—ICCP System 1994. Int J Coal Geol 169:40–61

Plumstead EP (1961) Ancient plants and drifting continents. S Afr J Sci 57(7):173–181

Qiu N, Li H, Jin Z, Zhu Y (2007) Temperature and time effect on the concentrations of free radicals in coal: evidence from laboratory pyrolysis experiments. Int J Coal Geol 69:220–228

Retcofsky HL, Stark JM, Friedel RA (1968) Electron spin resonance in American coals. Anal Chem 40(11):1699–1704

Retcosfky HL, Hough MR, Maguire MM, Clarkson RB (1981) Nature of the free radicals in coals, pyrolyzed coals, solvent-refined coal, and coal liquefaction products. In: Gorbaty ML, Ouchi K (eds) Coal structure, advances in chemistry, vol 192. American Chemical Society, Washington, DC, pp 37–58

Richardson AR, Eble CF, Hower JC, O'Keefe JMK (2012) A critical re-examination of the petrology of the No. 5 Block coal in eastern Kentucky with special attention to the origin of inertinite macerals in the splint lithotypes. Int J Coal Geol 98:41–49

Ruckwied K, Götz AE, Jones P (2014) Palynological records of the Permian Ecca Group (South Africa): utilizing climatic icehouse–greenhouse signals for cross basin correlations. Palaeogeogr Palaeoclimatol Palaeoecol 413:167–172

Scott AC (1989) Observations on the nature and origin of fusain. Int J Coal Geol 12:443–475

Scott AC (2002) Coal petrology and the origin of coal macerals: a way ahead? Int J Coal Geol 50:119–134

Scott AC (2010) Charcoal recognition, taphonomy and uses palaeoenvironmental analysis. Palaeogeogr Palaeoclimatol Palaeoecol 291:11–39

Scott AC, Glasspool IJ (2007) Observations and experiments on the origin and formation of inertinite group macerals. Int J Coal Geol 70(1–3):53–66

Silbernagel BG, Gebhard LA, Dyrkacz GR (1984a) Electron spin resonance of isolated coal macerals. In: Petrakis L, Fraissard JP (eds) Magnetic resonance. Introduction, advanced topics and applications to fossil energy. D. Reidel Publishing Company, Dordrecht, pp 645–653

Silbernagel BG, Gebhard LA, Dyrkacz GR, Bloomquist CAA (1984b) Electron spin resonance of isolated coal macerals, preliminary survey. In: Winans RE, Crelling JC (eds) Chemistry and characterization of coal macerals. ACS Symposium Series. American Chemical Society, Washington, DC, pp 121–135

Silbernagel BG, Gebhard LA, Dyrkacz GR, Bloomquist CAA (1986) Electron spin resonance of isolated coal macerals. Fuel 65:558–565

Slater BJ, McLoughlin S, Hilton J (2015) A high-altitude Gondwana lagerstätte: the Permian permineralised peat biota of the Prince Charles Mountains, Antarctica. Gondwana Res 27:1446–1473

Snyman CP (1989) The role of coal petrography in understanding the properties of South African coal. Int J Coal Geol 14:83–101

Solum MS, Pugmire RJ, Grant DM (1989) ^{13}C Solid-state NMR of Argonne Premium Coals. Energy Fuels 3:187–193

South African National Standards (SANS) 334:1992 (ISO 334:1992) Solid mineral fuels—determination of total sulfur—Eschka method

South African National Standards (SANS) 17247:2006 (ISO 17247:2005) Coal—ultimate analysis

South African National Standards (SANS) 1928:2009 (ISO 1928:2009) Solid mineral fuels—determination of gross calorific value by the bomb calorific method, and calculation of net calorific value

South African National Standards (SANS) 7936:2010 (ISO 7936:1992) Hard coal—determination and presentation of float and sink characteristics—general directions for apparatus and procedures

South African National Standards (SANS) 17246:2011 (ISO 17246:2010) Coal—proximate analysis

South African National Standards (SANS) 7404-2:2015 (ISO 7404-2:2009) Methods for the petrographic analysis of coals Part 2: methods of preparing coal samples

South African National Standards (SANS) 7404-3:2016 (ISO 7404-3:2009) Methods for the petrographic analysis of coals—Part 3: method of determining maceral group

Suggate RP, Dickinson WW (2004) Carbon NMR of coals: the effects of coal type and rank. Int J Coal Geol 57:1–22

Taylor GH, Teichmüller M, Davis A, Diessel CFK, Littke R, Robert P (1998) Organic petrology. Gebrüder Borntraeger, Berlin, p 704

Teichmüller M (1989) The genesis of coal from the viewpoint of coal petrology. In: Lyons PC, Alpern B (eds) Peat and coal: origin, facies, and depositional models. Int J Coal Geol 12:1–87

Van Niekerk D, Mathews JP (2010) Molecular representations of Permian-aged vitrinite-rich and inertinite-rich South African coals. Fuel 89:73–82

Van Niekerk D, Pugmire RJ, Solum MS, Painter PC, Mathews JP (2008) Structural characterization of vitrinite-rich and inertinite-rich Permian-aged South African bituminous coals. Int J Coal Geol 76:290–300

White A, Davies MR, Jones SD (1989) Reactivity and characterization of coal maceral concentrates. Fuel 68:511–519

Więckowski AB, Wojtowicz W, Pilawa B (2000) EPR characteristics of petrographically complex coal samples from durain and clarain. Fuel 79:1137–1141

Zhou Q, Liu Q, Shi L, Yuxin Y, Liu Z (2017) Behaviors of coking and radicals during reaction of volatiles generated from fixed-bed pyrolysis of a lignite and a subbituminous coal. Fuel Process Technol 161:304–310